Analysis of Closed Section Thin-walled Beams Subjected to Partially Restrained Warping

J. Ergatoudis

J. Nuttall

T. H. G. Megson

ANALYSIS OF CLOSED SECTION THIN-WALLED BEAMS SUBJECTED TO PARTIALLY RESTRAINED WARPING

T.H.G. Megson, J. Ergatoudis and J. Nuttall

1. INTRODUCTION

In many structures, for example grillages, ladder frames and some skeletal structures, closed section thin-walled beams are subjected to torsion which causes warping of cross-sections. At joints, where for example, the end of a closed section subsidiary beam is attached to the flexible web of an open or closed section main beam this warping is only partially restrained. This partial restraint modifies the displacements and stresses which would be predicted by assuming either completely free or completely restrained warping. In addition, in the absence of stiffening diaphragms, cross-sections of the subsidiary beam distort from their original shape and further modification of displacements and stresses occurs.

A finite element analysis of a complete main/subsidiary beam joint is capable of giving estimates of displacements and stresses. However, it has been found (1) that values of subsidiary beam stresses estimated in this manner are not in agreement with measured values at beam sections away from the partially restrained end.

This paper shows that these stresses may be estimated accurately by employing a variational method proposed by Vlasov (5); the resulting differential equations are solved by a finite difference technique described by Rao, Ramamurti and Ganesan (4). In the solution, boundary conditions at the partially restrained end of the subsidiary beam are determined by a finite element analysis.

2. THEORETICAL ANALYSIS

The present work is a development of that begun by Megson, Ergatoudis and Nuttall (1) who showed that the effective torsion constant for a closed section subsidiary member is independent, to a measurable accuracy, of the type of constraint applied at one end. They also showed that stresses predicted by theory which assumes an undistorted cross-section although giving good agreement with measured values in the region of the constraint does not give accurate estimates at sections away from the constraint. To allow for the effects of cross-sectional distortion Vlasov's variational method (5) is used.

T.H.G. Megson, Senior Lecturer in Civil Engineering, University of Leeds.
J. Ergatoudis, Lecturer in Civil Engineering, University of Leeds.
J. Nuttall, PAFEC Ltd., Nottingham.

2.1 Vlasov's Variational Method

The basis of Vlasov's method is that the axial and tangential components of displacement, u(z, s) and v(z, s), of any point (z, s) on the middle surface of a thin-walled beam may be represented in the form of a finite series; z is measured along the axis of the beam and s round the profile of the beam section. Thus:

$$u(z,s) = \sum_{i=1}^{m} U_i(z)\ \phi_i(s) \qquad (i = 1, 2, \ldots, m) \tag{1}$$

$$v(z,s) = \sum_{k=1}^{m} V_k(z)\ \psi_k(s) \qquad (k = 1, 2, \ldots, n) \tag{2}$$

where $\phi_i(s)$ and $\psi_k(s)$ are given functions of s, m is the number of nodal points in the section having m degrees of freedom with respect to longitudinal displacements and n is the number of degrees of freedom of the thin-walled beam in the plane of its cross-section. It may be shown (5) that n = 2m - c in which c is the number of walls comprising a multiply connected section. For a rectangular section beam c = m = 4 so that n = 4.

The functions ϕ_i (s) and ψ_k (s) are chosen initially to correspond to the displacement modes produced by different load applications. Thus, in Fig. 1, for a rectangular section beam, ϕ_1 corresponds to axial stretching, ϕ_2 and ϕ_3 to bending in two principal planes and ϕ_4 to warping. The tangential displacement functions are ψ_1 rotation, ψ_2 and ψ_3 translation along the two principal axes and ψ_4 distortion of the cross-section. Hence, referring to Fig. 1:

$$\left.\begin{aligned} &\phi_1(s) = 1,\ \phi_2(s) = x(s),\ \phi_3(s) = y(s),\ \phi_4(s) = x(s)y(s) \\ &\psi_1(s) = h(s),\ \psi_2(s) = x'(s),\ \psi_3(s) = y'(s),\ \psi_4(s) = x'(s)y(s) + x(s)y'(s) \end{aligned}\right\} \tag{3}$$

From Hooke's law, the direct stress is given by

$$\sigma(z,s) = E\frac{\partial u}{\partial z} \tag{4}$$

and the shear stress by

$$\tau(z,s) = G\left(\frac{\partial u}{\partial s} + \frac{\partial v}{\partial z}\right) \tag{5}$$

Substituting for u and v from eqns. (1) and (2) into eqns. (4) and (5) gives

$$\sigma(z,s) = E\sum_{i=1}^{m} U_i'(z)\ \phi_i(s) \qquad (i = 1, 2, \ldots, m) \tag{6}$$

and

$$\tau(z,s) = G\left[\sum_{i=1}^{m} U_i(z)\ \phi_i'(s) + \sum_{k=1}^{m} V_k'(z)\ \psi_k(s)\right] \quad \left(\begin{matrix} i = 1, 2, \ldots, m \\ k = 1, 2, \ldots, n \end{matrix}\right) \tag{7}$$

Consider now an elemental length, δz, of a beam and an element of width δs in a wall (Figs. 2(a) and (b)). The element is subjected to external forces p and q and internal stresses as shown. The length of beam has m + n degrees of freedom for the chosen displacements $\phi_i(s)$ and $\psi_k(s)$ so that using the principle of virtual displacements equilibrium conditions may be written as follows:

$$\oint \frac{\partial \sigma}{\partial z} \phi_j \, t ds - \oint \tau \phi_j' \, t ds + \oint p \phi_j \, ds = 0 \qquad (j = 1, 2, \ldots, m) \qquad (8)$$

$$\oint \frac{\partial \tau}{\partial z} \psi_h \, t ds - \Sigma V_k \oint \frac{M_k M_h}{EI} ds + \oint q \psi_h \, ds = 0 \qquad (h = 1, 2, \ldots, n) \qquad (9)$$

Equations (8) are the m equilibrium conditions of the length δz of the beam in the direction of the displacement u while eqns. (9) are the n equilibrium conditions corresponding to the tangential displacement modes (see reference 5).

Substituting for $\sigma(z,s)$ from eqn. (6) and $\tau(z,s)$ from eqn. (7) into eqns. (8) and (9) gives m + n differential equations for the displacements $U_i(z)$ and $V_k(z)$, i.e.

$$\frac{E}{G} \sum_{i=1}^{m} a_{ji} U_i'' - \sum_{i=1}^{m} b_{ji} U_i - \sum_{k=1}^{n} C_{jk} V_k' + \frac{p_j}{G} = 0 \qquad (10)$$

$$\sum_{i=1}^{m} c_{hi} U_i' + \sum_{k=1}^{n} r_{hk} V_k'' - \frac{E}{G} \sum_{k=1}^{n} s_{hk} V_k + \frac{q_h}{G} = 0 \qquad (11)$$

in which

$$a_{ji} = \oint \phi_j(s) \, \phi_i(s) \, t(s) \, ds, \qquad b_{ji} = \oint \phi_j'(s) \, \phi_i'(s) \, t(s) \, ds$$

$$c_{jk} = \oint \phi_j'(s) \, \psi_k(s) \, t(s) \, ds, \qquad c_{hi} = \oint \psi_h(s) \, \phi_i'(s) \, t(s) \, ds$$

$$r_{hk} = \oint \psi_h(s) \, \psi_k(s) \, t(s) \, ds, \qquad s_{hk} = \frac{1}{E} \oint \frac{M_h(s) \, M_k(s)}{EI} ds$$

Simplifying eqns. (10) and (11) for the case of a rectangular section beam of depth a, width b and corresponding wall thicknesses t_a and t_b results in eight differential equations of which three are independent and form a symmetrical system relating to warping (ϕ_4), rotation (ψ_1) and distortion (ψ_4). Writing $U_4 = w$, $V_1 = \theta$ and $V_4 = \gamma$ the equations become

$$\left.\begin{aligned} a_1 w'' - b_1 w - b_2 \theta' - b_1 \gamma + p_4 &= 0 \\ b_2 w' + b_1 \theta'' + b_2 \gamma'' + q_1 &= 0 \\ b_1 w' + b_2 \theta'' + b_1 \gamma'' - c_1 \gamma + q_4 &= 0 \end{aligned}\right\} \qquad (12)$$

$$\left.\begin{aligned} \text{in which } a_1 &= Ea^2b^2(at_a + bt_b)/24, \quad b_1 = Gab(at_b + bt_a)/2 \\ b_2 &= Gab(bt_a - at_b)/2, \quad c_1 = 8E/(a/t_a^3 + b/t_b^3) \end{aligned}\right\} \tag{13}$$

The external forces in eqns. (12) are

$$p_4 = \oint p\ \phi_4\ ds,\ q_h = \oint q\ \psi_h\ ds\ (h = 1,\ 4)$$

In accordance with the generalized coordinates shown in Fig. 1, p_4 is the applied longitudinal bimoment per unit length, q_1 the external torque per unit length and q_4 the external transverse or cross-bimoment per unit length.

Again using the concept of virtual work the internal bimoment B, torque T and cross-bimoment C_b may be expressed as

$$B = -\oint \sigma\ \phi_4\ tds, \qquad T = \oint \tau\ \psi_1\ tds, \qquad C_b = \oint \tau\ \psi_4\ tds \tag{14}$$

Substitution in eqns. (14) for σ and τ from eqns. (6) and (7) and simplifying for the case of a rectangular section beam gives

$$\left.\begin{aligned} B &= -a_1\ w' \\ T &= b_2\ w + b_1\ \theta' + b_2\ \gamma' \\ C_b &= b_1\ w + b_2\ \theta' + b_1 \gamma' \end{aligned}\right\} \tag{15}$$

Solution of eqns. (12) gives the three displacement functions and their derivatives; direct and shear stresses then follow by substitution in eqns. (6) and (7).

Additional direct stresses occur due to the distortion of the beam section and are produced by bending moments, M, in the individual plate elements (Fig. 3(a)). These stresses vary through the thickness as shown in Fig. 3(b) and are given by

$$\sigma_T(z) = \frac{M(z)y}{I}$$

where $M(z) = 12\gamma(z)/(a/EI_a + b/EI_b)$ (see reference (5)) and $I_a = t_a^3/12$, $I_b = t_b^3/12$ are the second moments of area per unit length of the beam web and cover respectively. The maximum transverse stress in the extreme fibre is then

$$\sigma_T(z) = \frac{12M(z)}{t^2}$$

where t is the smaller of t_a and t_b.

2.2 Solution by the Finite Difference Method

The differential equations (12) are rewritten in matrix form as (4)

$$RZ'' + SZ' + TZ = e \tag{16}$$

where R, S and T are 3 x 3 matrices containing the appropriate coefficients and

$$Z = \begin{Bmatrix} w \\ \theta \\ \gamma \end{Bmatrix}, \qquad e = \begin{Bmatrix} p_4 \\ q_1 \\ q_4 \end{Bmatrix}$$

Equation (16) is written in finite difference form at all locations by the use of a central difference formula except at the first and last locations which form the boundary conditions, thus

$$Z_i'' = \frac{Z_{i+1} - 2Z_i + Z_{i-1}}{\Delta^2}, \qquad Z_i' = \frac{Z_{i+1} - Z_{i-1}}{2\Delta}$$

where Δ is the interval between adjacent stations. The differential equations satisfying the boundary conditions may be written as

$$SZ' + TZ = e$$

which are also written in finite difference form, backward or forward difference formulae being used.

The finite difference equations along the length of the beam at each station, can be written as the following set of algebraic equations in Z,

$$\left.\begin{aligned} &A_oZ_1 + B_oZ_o = g_o \\ &A_iZ_{i+1} + B_iZ_i + C_iZ_{i-1} = g_i \quad (i = 1, 2, \ldots, n-1) \\ &B_nZ_n + C_nZ_{n-1} = g_n \end{aligned}\right\} \tag{17}$$

where A, B and C are 3 x 3 matrices, g is a 3 element column vector and

$$A_o = S_o/\Delta, \quad B_o = T_o - S_o/\Delta, \quad g_o = e_o$$

$$A_i = 2R_i/\Delta + S_i, \quad B_i = -4R_i/\Delta + 2\Delta T_i, \quad C_i = 2R_i/\Delta - S_i \quad (i = 1, 2, \ldots, n-1)$$

$$g_i = 2\Delta e_i, \quad B_n = T_n + S_n/\Delta, \quad C_n = -S_n/\Delta, \quad g_n = e_n$$

Equations (17) were solved for the cases specified in Section 4 by the Gauss elimination method programmed using the high level language ALGOL 68R for execution on the Leeds 1906A computer (3).

2.3 Boundary Conditions

The boundary conditions for the solution of any beam problem by the above method depend upon the support and loading conditions at the ends of the beam although additional boundary conditions may be applied at any station along the beam. Boundary conditions may be in the form of prescribed displacements, applied loads or a combination of both.

In the case of applied loads at the ends of the beam the relevant equation in eqns. (15) replaces that in eqns. (12) corresponding to the displacement mode the applied load would induce. For the case of an applied load at an internal station eqns. (12) are used but the relevant value of p_4, q_1 or q_4 is included. Thus if a bimoment B, torque T and cross-bimoment C_b are applied then

$$p_4 = B/\Delta, \qquad q_1 = T/\Delta, \qquad q_4 = C_b/\Delta$$

For the present investigation in which a pure torque is applied to the free end of the subsidiary member

$$p_4 = B = 0, \qquad q_1 = T/\Delta, \qquad q_4 = C_b = 0$$

Known values of displacement at a station are also included by replacing the relevant equation in eqns. (12) by variable (w, θ, γ) = known value. Thus at a fully clamped end $w = \theta = \gamma = 0$. In the case of partially restrained warping the rotation θ may be fixed at zero at the partially restrained end to provide a datum for the angle of twist along the length of the subsidiary member. However, the warping w and distortion γ will have values of which w can only be found by a finite element analysis of the particular joint configuration under investigation.

The distortion γ of the subsidiary beam cross-section at the partially restrained end is a function of the tangential displacement of a point on a wall which is parallel to the axis of the main beam. This tangential displacement is composed of the rotation of the section due to the applied torque and distortion of the section due to warping of the main beam cross-section. This warping is caused by the torque in the subsidiary beam acting as a moment in the main beam web and thereby inducing a bimoment. In this case the distortion is most accurately found from a finite element analysis but can, alternatively, be calculated (2).

3. FINITE ELEMENT ANALYSIS

Three joints, each consisting of a channel section main member and a closed rectangular section subsidiary member were analysed using the finite element method to determine the required boundary conditions at the partially restrained end; the dimensions of the different joints are given in Table 1, Section 4. Eight node isoparametric quadrilateral elements which combine both bending and membrane properties were used; a typical idealisation is shown in Fig. 4

The vertical edges of the main beam were restrained such that vertical displacements and displacements perpendicular to its web were prevented. The torque was applied to the free end of the subsidiary member in the form of couples comprising horizontal and vertical loads P and Q (Fig. 4). To eliminate the distortional action of the couples P and Q were proportioned such that the cross-bimoment due to P and Q was zero, thus $P/Q = a/b$ (see reference (2)).

The idealised structure was analysed using sub-routines from the Program for Automatic Finite Element Calculation known as PAFEC (5). The output from the program lists values of displacement and rotation at each node so that the boundary conditions required in the theoretical analysis are readily obtained. Stress distributions, rotations and warping displacements were then calculated as outlined in Section 2 for each of the joints listed in Table 1.

4. EXPERIMENTAL INVESTIGATION

Three joints were constructed using mild steel channel section main members and mild steel rectangular section subsidiary members. The nominal dimensions of each joint are listed in Table 1.

Table 1

Joint Number	Main Member web	Main Member flanges	Subsidiary Member web	Subsidiary Member flanges
1	197 x 3.2 mm (7.8 x 0.125 in)	102 x 3.2 mm (4 x 0.125 in)	95 x 4.8 mm (3.75 x 0.19in)	44 x 4.8 mm 1.75 x 0.19 in)
2	197 x 6.4 mm (7.8 x 0.25 in)	98 x 6.4 mm (3.9 x 0.25 in)	146 x 4.8 mm (5.75 x 0.19 in)	71 x 4.8 mm (2.8 x 0.19 in)
3	197 x 6.4 mm (7.8 x 0.25 in)	95 x 6.4 mm (3.75 x 0.25 in)	95 x 4.8 mm (3.75 x 0.19 in)	44 x 4.8 mm (1.75 x 0.19 in)

The experimental arrangement is shown diagrammatically in Fig. 5 where the main member web is bolted at each end along its centre line to vertical columns. Since high values of torque were required to produce measurable displacements loads were applied to each end of two cylindrical bars which passed through holes placed as close as possible to the free end of the subsidiary beam. The holes were positioned on the axes of symmetry of the section to coincide with points of zero warping thereby minimising local constraint effects. Stresses were obtained from strain readings of electrical resistance strain gauges placed at suitable positions along the length of the subsidiary member. Rotations were measured using a 'Talyrel' electronic level which was accurate to ± 20 seconds of arc.

Figures 6, 7, 8, 9 and 10 show typical distributions of the different parameters obtained both analytically using Vlasov's method and experimentally. In Fig. 6, however, only the theoretical distribution of warping is shown since warping displacements are too small to be measured with any degree of accuracy.

Figure 7 shows the close agreement obtained between measured and theoretical values of rotation. Figures 8 and 9 compare measured and theoretical values of axial and transverse direct stress along one edge of the subsidiary beam, again close agreement is obtained. It can be seen from Fig. 9 that the loading mechanism employed in the experimental analysis produces a high degree of distortion. However, by applying the appropriate boundary conditions at the loaded section it is seen that Vlasov's theory is capable of allowing for this.

CONCLUSIONS

It has been shown that Vlasov's variational theory, when combined with boundary conditions obtained by the finite element method, is capable of accurately predicting rotations and stresses in closed rectangular section members subjected to partially restrained warping. Furthermore the method is fully capable of allowing for the distortional effects produced by particular forms of loading.

Appendix 1: References

1. Megson, T.H.G., Ergatoudis, J. and Nuttall, J., "Partially Restrained Warping of Open and Closed Section Thin-Walled Beams", Proc. of the International Conference on Thin-Walled Structures, University of Strathclyde, April 1979.

2. Nuttall, J., "Structural Analysis of Ladder Frames under Torsion", Thesis submitted in partial fulfilment of the requirements for Ph.D., Univ. of Leeds, 1980.

3. PAFEC 75, Manual for the Program for Automatic Finite Element Calculations, PAFEC Ltd., Nottingham, 1976.

4. Rao, B.V.A., Ramamurti, V. and Ganesan, N., "Torsion of Prismatic Shells by Finite Difference Approach", Jour. of Aero Soc. of India, Vol. 25, 1973.

5. Vlasov, V.Z., "Thin-Walled Elastic Beams", Israel Program for Scientific Translations, Jerusalem, 1959.

Appendix 2: Notation

a - depth of beam section web
B - bimoment
b - width of beam section cover
C_b - cross-bimoment
c - number of walls in beam section
E - Young's modulus
G - shear modulus
I - second moment of area
M - bending moment
m - number of longitudinal degrees of freedom
n - number of tangential degrees of freedom
P - component of applied couple
p - external force in z direction
Q - component of applied couple
q - external force in s direction
s - distance round profile of beam section to any point
T - torque
t - wall thickness
t_a - thickness of webs
t_b - thickness of covers
$U(z)$ - longitudinal displacement function
u - longitudinal displacement
$V(z)$ - tangential displacement function
v - tangential displacement
w - warping displacement
x, y - principal axes of beam section
z - longitudinal axis of beam
γ - distortion of beam section
Δ - interval between beam stations
θ - rotation
σ - direct stress
τ - shear stress
$\phi(s)$, $\psi(s)$ - prescribed displacement functions

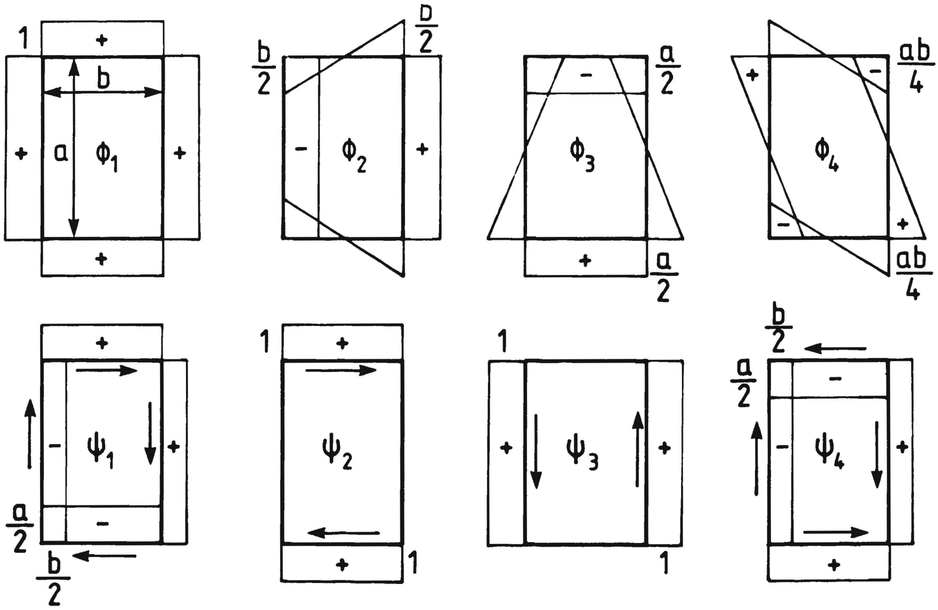

Fig. 1 Displacement functions for a rectangular section beam

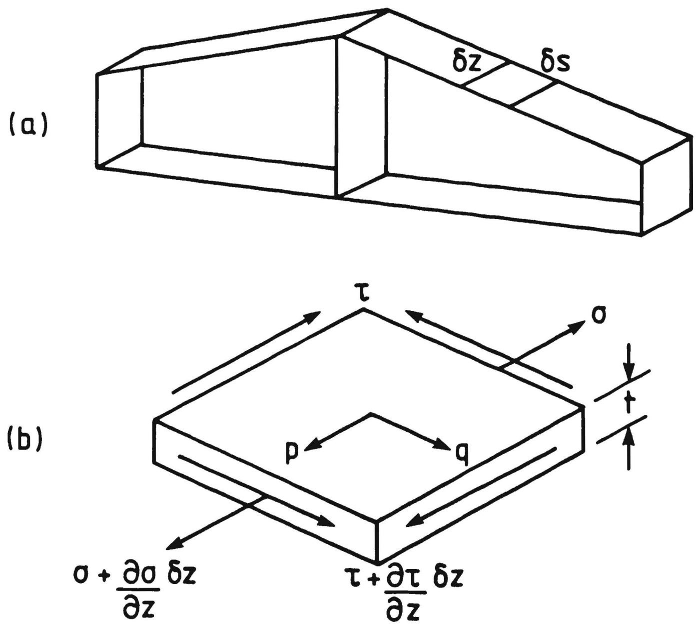

Fig. 2 Equilibrium of elemental length of beam

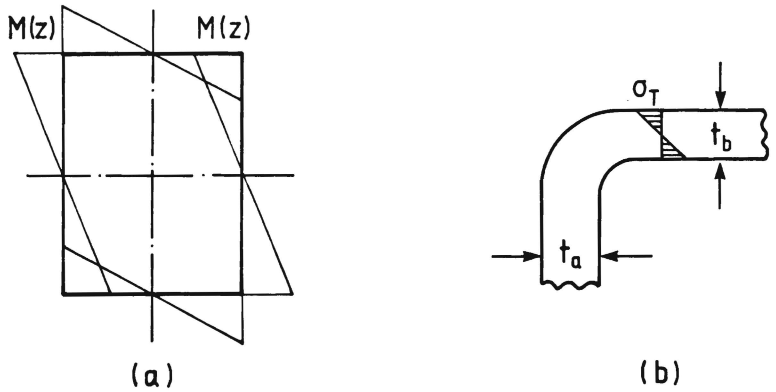

Fig. 3 Transverse stress due to distortion of beam section

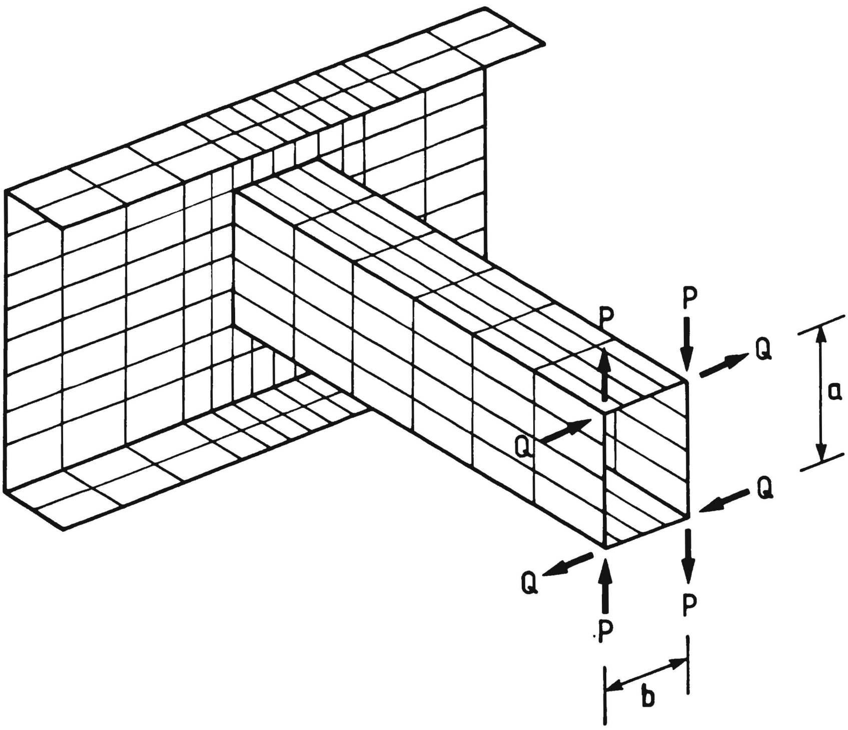

Fig. 4 Typical finite element mesh and method of load application

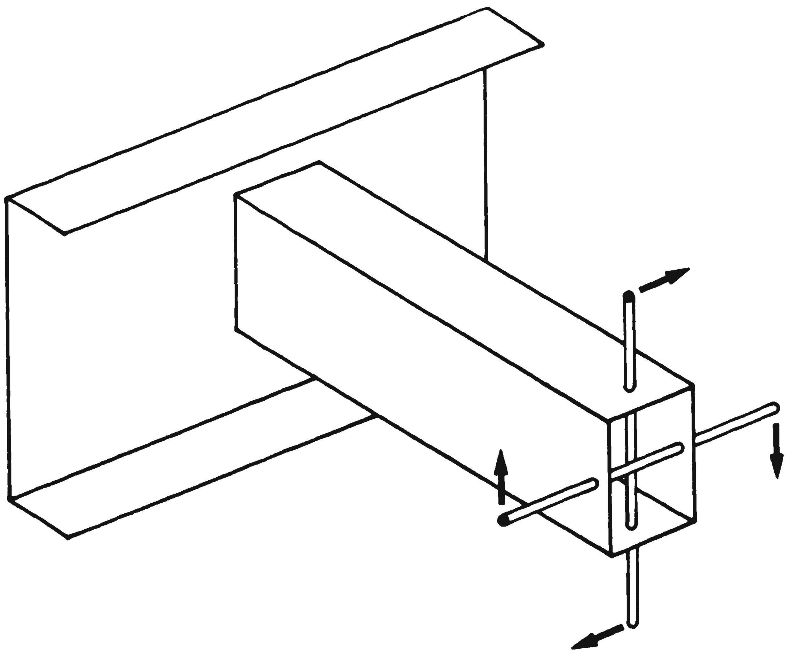

Fig. 5 Method of load application (experimental)

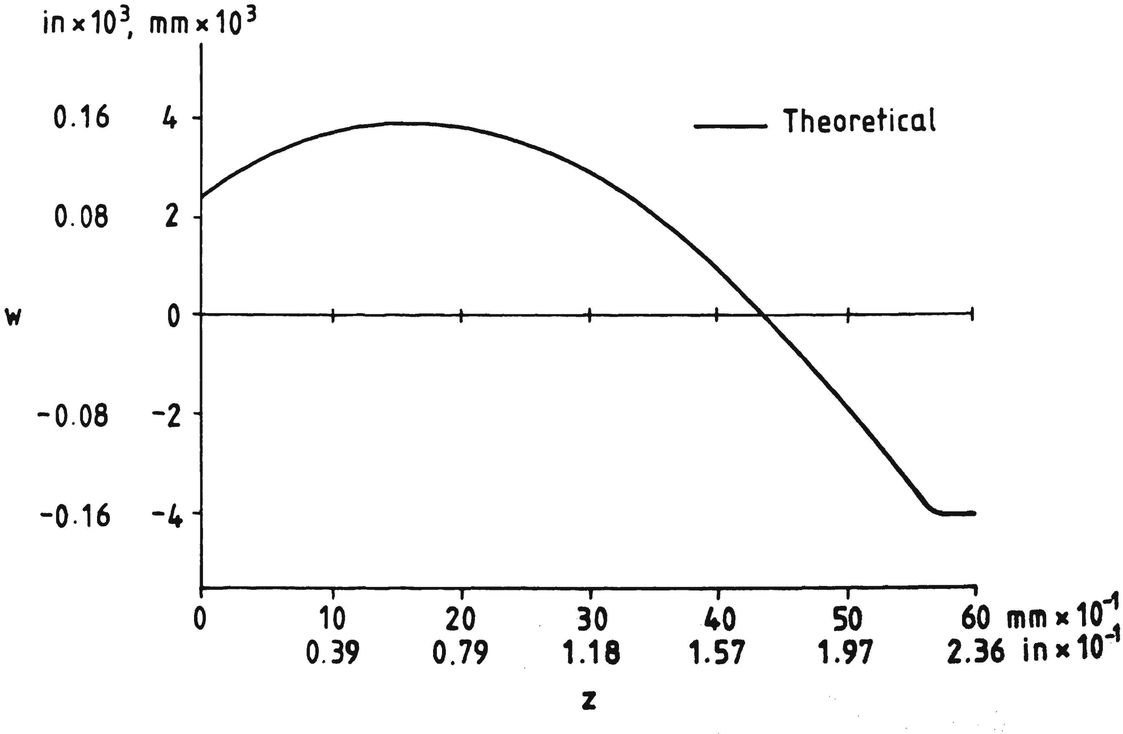

Fig. 6 Warping distribution along length of subsidiary beam

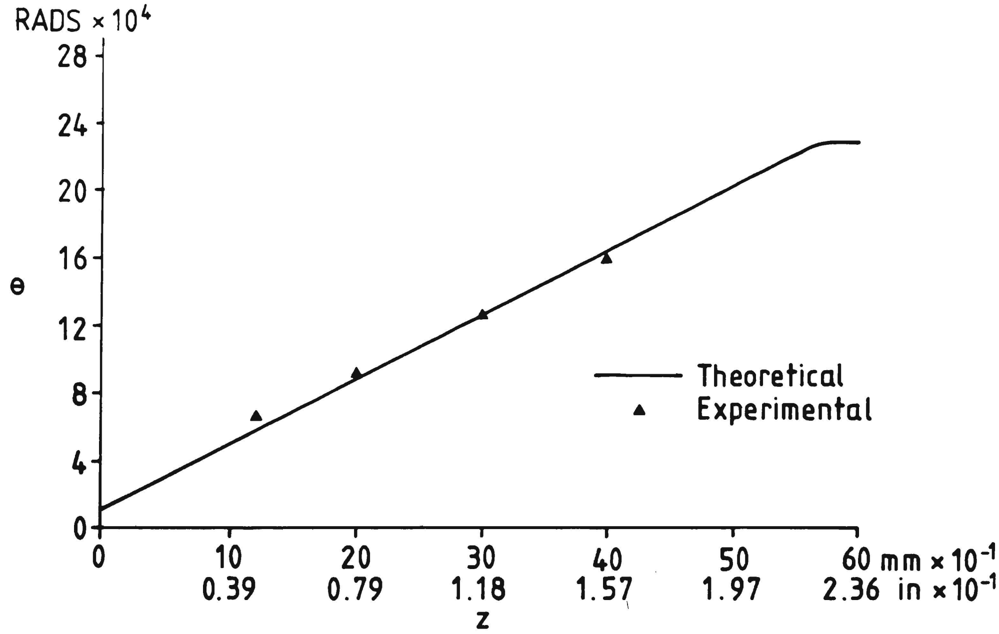

Fig. 7 Rotation along length of subsidiary beam

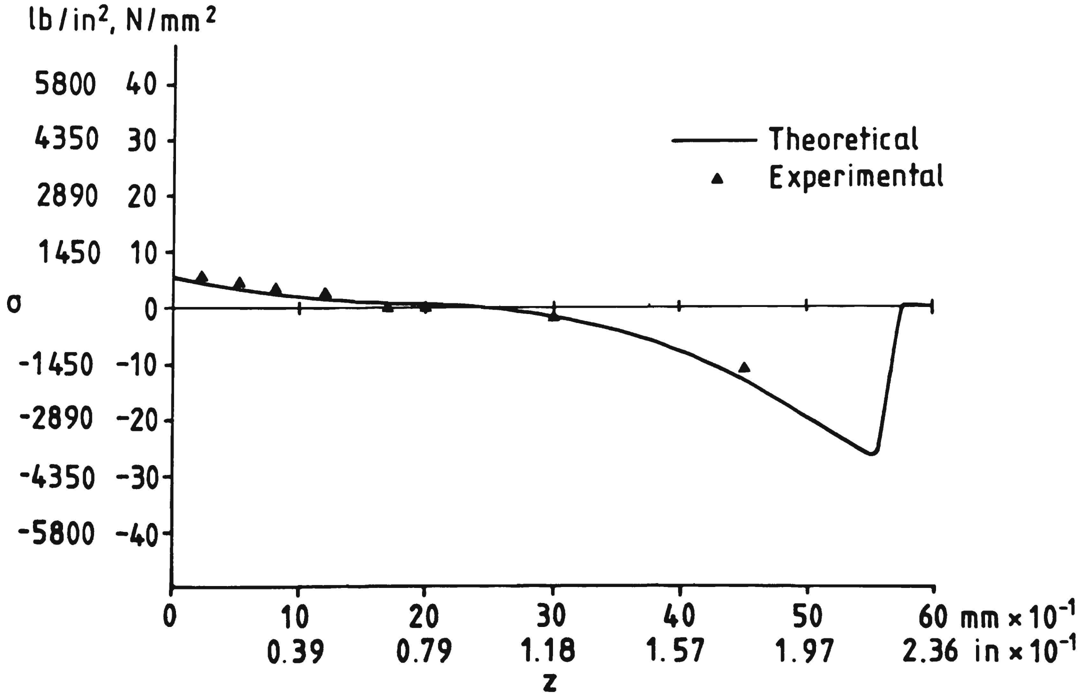

Fig. 8 Distribution of longitudinal direct stress along length of subsidiary beam

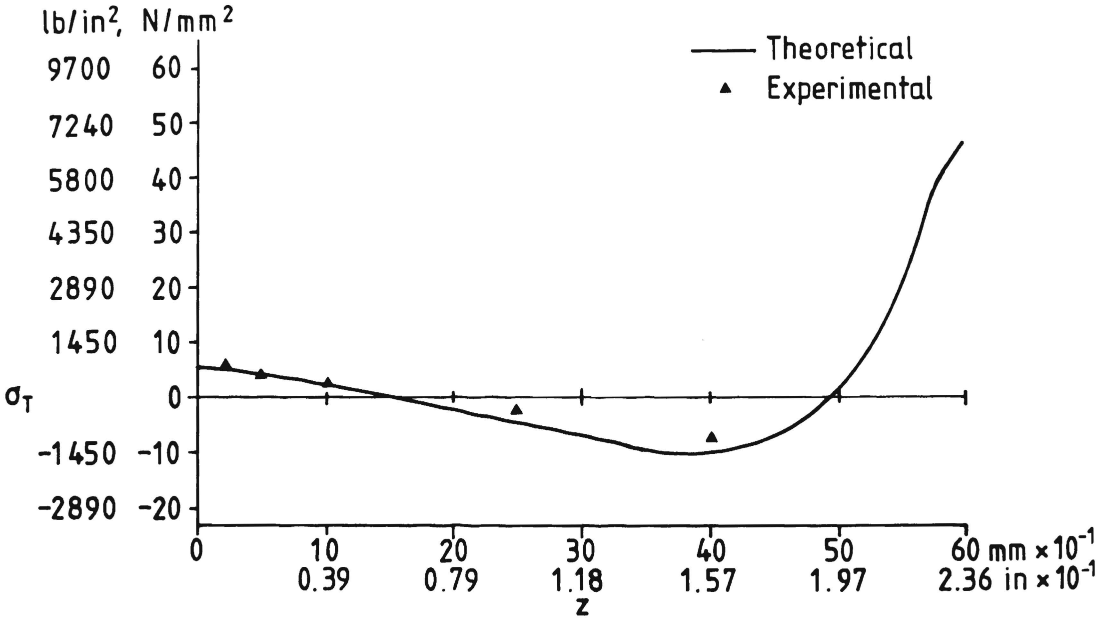

Fig. 9 Distribution of transverse direct stress along length of subsidiary beam.

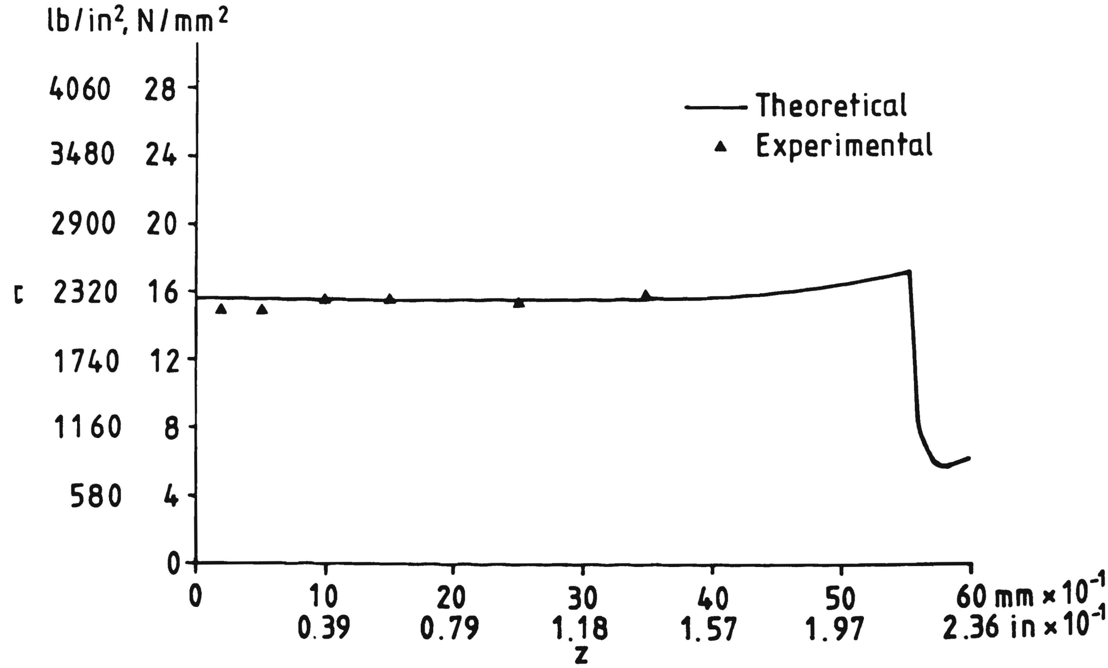

Fig. 10 Distribution of shear stress along length of subsidiary beam.